Supplemental material to this article can be found at:
http://jpet.aspetjournals.org/content/suppl/2021/02/01/jpet.120.000365.DC1

1521-0103/377/1/108–120$35.00
THE JOURNAL OF PHARMACOLOGY AND EXPERIMENTAL THERAPEUTICS
Copyright © 2021 by The American Society for Pharmacology and Experimental Therapeutics
https://doi.org/10.1124/jpet.120.000365
J Pharmacol Exp Ther 377:108–120, April 2021

The Journal of PHARMACOLOGY And Experimental Therapeutics

A Novel Mitochondrial Complex of Aldosterone Synthase, Steroidogenic Acute Regulatory Protein, and Tom22 Synthesizes Aldosterone in the Rat Heart[S]

Himangshu S. Bose, Randy M. Whittal, Brendan Marshall, Maheshinie Rajapaksha, Ning Ping Wang, Madhuchanda Bose, Elizabeth W. Perry, Zhi-Qing Zhao, and Walter L. Miller

Biomedical Sciences, Mercer University School of Medicine, Savannah, Georgia (H.S.B., M.R., N.P.W., Z.-Q.Z.); Department of Chemistry, University of Alberta, Edmonton, Alberta, Canada (R.M.W.); Department of Cellular Biology and Anatomy, Medical College of Georgia, Augusta University, Georgia (B.M., E.W.P.); Curtiss Healthcare, University of Florida Innovate Sid Martin Biotechbology Incubator, Gainesville, Florida (M.B.); Anderson Cancer Institute, Savannah, Georgia (H.S.B.); and Department of Pediatrics and Center for Reproductive Sciences, University of California San Francisco, San Francisco, California (W.L.M.)

Received October 5, 2020; accepted January 25, 2021

ABSTRACT

Aldosterone, which regulates renal salt retention, is synthesized in adrenocortical mitochondria in response to angiotensin II. Excess aldosterone causes myocardial injury and heart failure, but potential intracardiac aldosterone synthesis has been controversial. We hypothesized that the stressed heart might produce aldosterone. We used blue native gel electrophoresis, immunoblotting, protein crosslinking, coimmunoprecipitations, and mass spectrometry to assess rat cardiac aldosterone synthesis. Chronic infusion of angiotensin II increased circulating corticosterone levels 350-fold and induced cardiac fibrosis. Angiotensin II doubled and telmisartan inhibited aldosterone synthesis by heart mitochondria and cardiac production of aldosterone synthase (P450c11AS). Heart aldosterone synthesis required P450c11AS, Tom22 (a mitochondrial translocase receptor), and the intramitochondrial form of the steroidogenic acute regulatory protein (StAR); protein crosslinking and coimmunoprecipitation studies showed that these three proteins form a 110-kDa complex. In steroidogenic cells, extramitochondrial (37-kDa) StAR promotes cholesterol movement from the outer to inner mitochondrial membrane where cholesterol side-chain cleavage enzyme (P450scc) converts cholesterol to pregnenolone, thus initiating steroidogenesis, but no function has previously been ascribed to intramitochondrial (30-kDa) StAR; our data indicate that intramitochondrial 30-kDa StAR is required for aldosterone synthesis in the heart, forming a trimolecular complex with Tom22 and P450c11AS. This is the first activity ascribed to intramitochondrial StAR, but how this promotes P450c11AS activity is unclear. The stressed heart did not express P450scc, suggesting that circulating corticosterone (rather than intracellular cholesterol) is the substrate for cardiac aldosterone synthesis. Thus, the stressed heart produced aldosterone using a previously undescribed intramitochondrial mechanism that involves P450c11AS, Tom22, and 30-kDa StAR.

SIGNIFICANCE STATEMENT

Prior studies of potential cardiac aldosterone synthesis have been inconsistent. This study shows that the stressed rat heart produces aldosterone by a novel mechanism involving aldosterone synthase, Tom22, and intramitochondrial steroidogenic acute regulatory protein (StAR) apparently using circulating corticosterone as substrate. This study establishes that the stressed rat heart produces aldosterone and for the first time identifies a biological role for intramitochondrial 30-kDa StAR.

Introduction

Aldosterone, which is synthesized in mitochondria of adrenal zona glomerulosa (ZG) cells, is the principal mineralocorticoid regulating renal sodium retention, thus influencing serum sodium, intravascular volume, and arterial blood pressure. Adrenal aldosterone synthesis is regulated by serum potassium, by the renin/angiotensin system, and by corticotropin (Hattangady et al., 2012) and may also be induced by

H.S.B. was previously supported by grants from National Institutes of Health [R01 Grant HD057876], Navicent Foundation [Grant 570257], and a seed grant from Mercer University.

No author has an actual or perceived conflict of interest with the contents of this article

https://doi.org/10.1124/jpet.120.000365.

[S] This article has supplemental material available at jpet.aspetjournals.org.

ABBREVIATIONS: AngII, angiotensin II; AT, angiotensin II receptor type; BS^3, bis(sulfosuccinimidyl)suberate; BSA, bovine serum albumin; co-IP, coimmunoprecipitation; COX IV, cytochrome oxidase complex IV; 2D, two-dimensional; DOC, deoxycorticosterone; EM, electron microscopy; ER, endoplasmic reticulum; IMM, inner mitochondrial membrane; LC-MS/MS, liquid chromatography followed by MS/MS; MAM, mitochondria-associated membrane; MS/MS, mass spectrometric analysis; NIH, National Institutes of Health; OMM, outer mitochondrial membrane; P450c11AS, aldosterone synthase; P450scc, cholesterol side-chain cleavage enzyme; RIA, radioimmunoassay; siRNA, small interfering RNA; StAR, steroidogenic acute regulatory protein; TEM, transmission EM; VDAC2, voltage-dependent access channel 2; ZG, zona glomerulosa.

Downloaded from jpet.aspetjournals.org at ASPET Journals on April 9, 2024

leptin (Huby et al., 2015). Renin, a serine protease secreted by renal juxtaglomerular cells, liberates the decapeptide angiotensin I from angiotensinogen, and then angiotensin-converting enzyme in the vasculature cleaves angiotensin I to the octapeptide angiotensin II (AngII). Four G-protein–coupled angiotensin receptors have been described (AT1-4), but AngII acts primarily via AT1 to stimulate production of phosphatidylinositol, mobilize intracellular and extracellular Ca^{2+}, and activate signaling via protein kinase C and the calcium-calmodulin system. Activation of AT1 directly stimulates aldosterone production and arteriolar constriction, with both raising blood pressure (Murphy et al., 1991; de Gasparo et al., 2000; Karnik et al., 2015). Aldosterone binds to the mineralocorticoid receptor, activating expression of genes involved in renal sodium and water reabsorption and potassium release. Hyperaldosteronism causes hypertension and cardiac fibrosis, a common cause of death (Gewirtz and Dilsizian, 2017). Although AT1 is found in the heart (Burson et al., 1994; Gasc et al., 1994) and its cardiac-specific overexpression in transgenic mice causes ventricular hypertrophy and heart failure (Paradis et al., 2000), it appears that aldosterone rather than AngII is principally responsible for myocardial injury (Rocha et al., 2000; Rocha et al., 2002; Cannavo et al., 2019).

In the adrenal, only ZG cells express AT1 (Jöhren et al., 2003; Premer et al., 2013) and aldosterone synthase (P450c11AS, CYP11B2) (Gomez-Sanchez et al., 2014), the mitochondrial enzyme specifically required for aldosterone synthesis (Curnow et al., 1991; Ogishima et al., 1991; Kawamoto et al., 1992). In ZG cell mitochondria, cholesterol is converted to progesterone by the sequential actions of the cholesterol side-chain cleavage enzyme (P450scc, CYP11A1) and 3β-hydroxysteroid dehydrogenase type 2, and then progesterone is 21-hydroxylated to deoxycorticosterone (DOC) by 21-hydroxylase (CYP21A2) in the endoplasmic reticulum (ER). DOC must re-enter the mitochondria where P450c11AS on the inner mitochondrial membrane (IMM) catalyzes the three reactions (11-hydroxylation, 18-hydroxylation, 18-methyl oxidation) that convert DOC to aldosterone (Miller and Auchus, 2011; Bose et al., 2020). Steroid-modifying 11β-hydroxysteroid dehydrogenase, type 2 is found in rodent and human heart (Walker et al., 1991; Lombès et al., 1995; Slight et al., 1996), and low levels of aldosterone have been reported in rat heart (Silvestre et al., 1998; Takeda et al., 2000). Furthermore, mRNAs for P450scc, 3β-hydroxysteroid dehydrogenase type 2, 21-hydroxylase, 11β-hydroxylase (CYP11B1), and 11β-hydroxysteroid dehydrogenase, type 2 are found in adult human heart, and mRNA for P450c11AS was found in the aorta and fetal human heart but not the adult heart (Kayes-Wandover and White, 2000). Nevertheless, controversy remains about cardiac steroidogenesis (Casal et al., 2003; Ye et al., 2005; MacKenzie et al., 2012). The steroidogenic acute regulatory protein (StAR), which facilitates the rapid delivery of cholesterol from the outer mitochondrial membrane (OMM) to P450scc on the matrix side of IMM in the adrenals and gonads (Lin et al., 1995; Bose et al., 2020), is also found in acutely stressed mouse heart (Anuka et al., 2013a,b). However, the heart lacks P450scc [Anuka et al. (2013b) and this paper], hence the role of cardiac StAR cannot be to increase mitochondrial cholesterol influx to serve as substrate for aldosterone synthesis.

AngII-induced hypertension and cardiac fibrosis are associated with locally upregulated AT1 receptor in the heart (Robert et al., 1999; Schnee and Hsueh, 2000; Murphy et al., 2015); suppressing the metabolism or action of aldosterone using an angiotensin-converting enzyme inhibitor, AT1 receptor blocker, or aldosterone receptor antagonist will reduce hypertension, cardiac hypertrophy, and fibrosis. To determine whether the chronically stressed heart can synthesize aldosterone, we studied cardiac P450c11AS, the rate-limiting enzyme in aldosterone metabolism, in rats receiving constant infusion of AngII.

Materials and Methods

Animals. We used our previously described rat model (Zhang et al., 2015). Male Sprague-Dawley rats (Envigo, Indianapolis, IN) weighing 200 ± 10 g were kept in a 12-hour light/dark cycle, 60% humidity, and temperature-controlled environment with standard rat chow and water ad libitum. The experimental protocols used in this study were approved by the Institutional Animal Care and Use Committee of Mercer University (A1707013). The current study was performed on rats that received implantation of osmotic minipumps. To avoid tissue injury induced by angiotensin II infusion with minipumps but not associated with minipump perfusion, in separate control group, minipumps were implanted, and saline was infused via the minipumps for the same length of time as the experimental rats received AngII. This specific group is defined as the sham group.

On the day of minipump implantation, rats were anesthetized in the morning with an intraperitoneal injection of a mixture of ketamine (90 mg/kg) and zylaxine (10 mg/kg), skin was swabbed with povidone-iodine and alcohol, and an incision was made between the scapulae. An osmotic minipump (model 2004; ALZET, Cupertino, CA) was inserted into the pocket (Zhang et al., 2015). Prior to implantation, the pumps were incubated overnight at 37°C with 0.9% sterile saline. Thirty-six rats (six in each group described below) were randomly assigned to six groups: 1) 2-week control (sham; these animals received osmotic pumps delivering saline for 2 weeks), 2) 4-week control; 3) 2 weeks AngII infusion [these animals received subcutaneous AngII (Sigma) at a rate of 500 ng/kg/min], 4) 4 weeks Ang II (delivered as above), 5) 2 weeks AngII plus telmisartan (Boehringer Ingelheim, Ridgefield CT) by gastric gavage at a dose of 10 mg/kg/day starting on the 2nd day after AngII minipump implantation, and 6) 4 weeks of AngII plus Telmi (delivered as above) (Fig. 1A). The aforementioned experiment with 36 rats was done four separate times (144 rats). The solution containing telmisartan was directly administered into the stomach of rats via an oral gavage. A stainless steel bulb-tipped gavage needle that was attached to a syringe was used to deliver the drug into the stomach. Gavage needles came in rat size and length. The half-life of telmisartan is approximately 24 hours when it is taken by mouth (Benson et al., 2004). At the end of the experiment, rats were euthanized with an overdose of anesthesia. No rats were lost during the experiments. The hearts were removed immediately and washed in cold Krebs-Henseleit solution [118 mM NaCl. 4.7 mM KCl, 1.2 mM $MgSO_4$, 1.25 mM $CaCl_2$, 1.2 mM KH_2PO_4, 10 mM HEPES (pH 7.4), 25 mM $NaHCO_3$, 11.1 mM glucose]. The left ventricle was obtained after removal of both atria and the free wall of the right ventricle. The left ventricular weight was determined as the sum of the free left ventricular wall weight and the interventricular septal weight, in which the average weight of the heart was 5.2 ± 0.5 g. Tissues were then frozen in liquid nitrogen and stored at −80°C until use. Usually 0.1–0.2 g of heart tissue was washed with PBS, incubated with 10 mM HEPES buffer (pH 7.4), and homogenized with 20 up-and-down stokes in a hand-held glass Dounce homogenizer, and the mitochondria were harvested and purified after our published procedures (Prasad *et al.*, 2017; Bose *et al.*, 2019).

Cell Culture. Rat myocardial H9c2 cells (ATCC CRL-1446) were grown at a density of ~10^5 cells/cm^2 and cultured as monolayers in 15-cm gelatin-coated plastic dishes in Dulbecco's modified Eagle's medium supplemented with fetal calf serum [10% (vol/vol)], glutamine (2 mM), essential amino acids (1%), and penicillin-streptomycin

Downloaded from jpet.aspetjournals.org at ASPET Journals on April 9, 2024

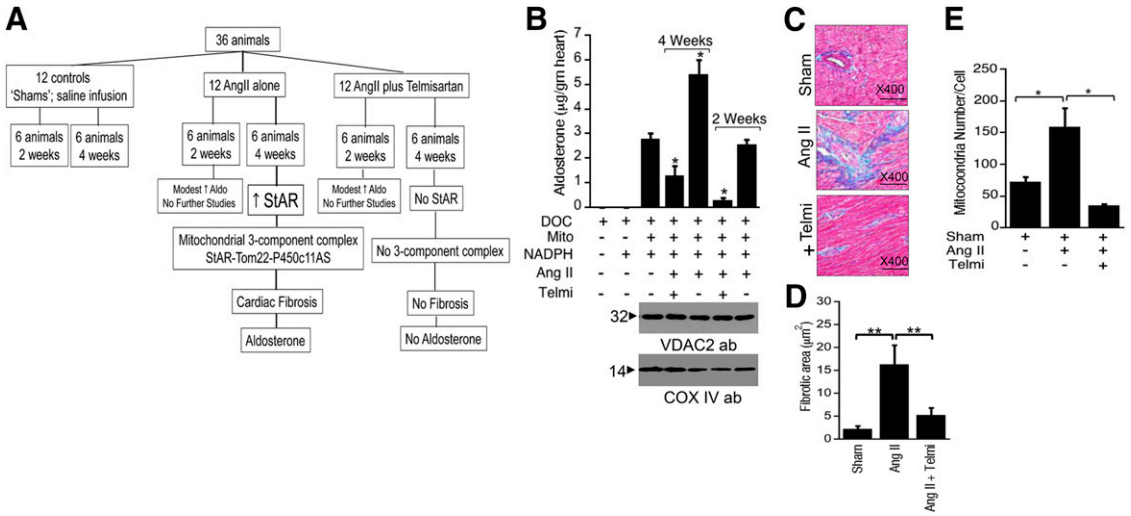

Fig. 1. Increased aldosterone synthesis with mitochondrial stress. (A) Flow diagram of the animal experiments. The 36 rats were divided into six groups, but we discontinued use of the animals treated for 2 weeks after the initial stages of the work. Four weeks treatment with AngII increased expression of StAR, increased formation of the StAR-Tom22-P450c11AS complex, induced cardiac fibrosis, and increased aldosterone (Aldo) biosynthetic capacity of isolated rat heart mitochondria. (B) Aldosterone synthesis in mitochondria (Mito) from rat heart tissue ($n = 6$ animals per group) after 2 or 4 weeks of angiotensin II infusion (AngII) in the absence and presence of telmisartan (Telmi). The reaction was initiated by adding tritiated DOC, the substrate for P450c11AS, and NADPH. The asterisk (*) indicates significant ($P < 0.001$) increase or decrease compared with the untreated control ($n = 9$). Bottom panels: immunoblots with VDAC2 and COX IV antibodies(ab) showing that each lane contains equivalent amounts of protein. (C) Representative images of Masson's trichrome staining showing cardiac fibrosis (blue). Top panel: untreated (sham-operated) heart; middle panel: AngII infusion for 4 weeks, resulting in extensive fibrosis; bottom panel: cotreatment with AngII and telmisartan for 4 weeks. (D) Quantitation of the area of myocardial fibrosis from the immunohistochemistry shown in (C). Eight randomized high-powered fields per tissue section were quantitated from six animals in each of the three groups (Sham, AngII, AngII plus Telmi). Infusion of AngII increased fibrosis significantly ($P < 0.05$, $n = 6$) compared with the sham control (*), and coadministration of telmisartan reduced the AngII-induced increase significantly ($P < 0.05$, $n = 6$) (*) but not back to the level of the untreated sham control. (E) Quantitation of mitochondrial number per cell after infusion of AngII in the presence and absence of Telmi. AngII increased the number of mitochondria per cell significantly (*$P < 0.001$), and coadministration of telmisartan decreased the AngII-mediated increase (*$P < 0.001$).

(100×) under a humidified atmosphere of 5% CO_2 at 37°C. COS-1 cells and mouse Leydig MA-10 cells were maintained as described without modification (Prasad et al., 2017). The medium was replaced with fresh medium every 2 days. Cells were treated with 50 nM human AngII for 24 hours (solubilized in water). Cells cotreated with telmisartan were first stimulated with AngII for 12 hours, which was followed by incubation with 20 μM telmisartan solubilized in DMSO for an additional 12 hours. StAR expression in H9c2 cells was knocked down via siRNA after transfection with equal amounts of the oligonucleotides (Forward 5′-GGAGAGUCAGCAGGACAAUtt-3′ and Reverse 5′-AUUGUCCUGCUGACUCUCCtt-3′) using oligofectamine (Thermo Fisher) as previously described (Bose *et al.*, 2008, 2019).

Immunohistochemistry and Masson's Trichrome Staining. Immunohistochemistry was performed on formalin-fixed and paraffin-embedded tissue. Tissue sections (6 μm) obtained with a Leica RM2135 microtome were dewaxed in xylene and rehydrated through graded alcohols. The sections were incubated overnight with primary antibodies, including a rabbit polyclonal anti-StAR antibody (Bose et al., 1999) [1:3000], a mouse monoclonal anti-Tom22 (Santa Cruz Biotech, Dallas, TX) [1:100], and our high-titer rabbit polyclonal anti-P450c11AS antibody (Adams and Bose, 2012) [1:2000]. The slides were then incubated with a biotinylated horse–anti-rabbit IgG or anti-mouse IgG [1:5000] (Vector Laboratories), stained using the ABC-peroxidase kit or ABC-AR (alkaline phosphatase; Vector Laboratories), and visualized with a 3,3′-diaminobenzidine tetrahydrochloride or alkaline phosphatase substrate kit (Sigma). The quality of the immunohistochemical assay was controlled by either elimination of the primary antibody or incubating the tissue with a nonimmune IgG. The expression of StAR, Tom22, and P450c11AS in the intracardiac vessels and intermyocardium was compared among groups using computer-assisted morphometry (400× magnification, ImageJ; NIH). Masson's trichrome staining was used to identify myocardial fibrosis through blue collagen staining. Images captured from eight randomized high-powered fields per tissue section were selected to determine the positively-stained collagen areas as square micrometer (400× magnification, ImageJ; NIH). The areas of fibrosis are expressed as mean ± S.E. A one-way ANOVA followed by Student-Newman-Keul's post hoc test was used to analyze group differences in the intensity of Western blot bands and the expression of immunohistochemical results for multiple comparisons using SigmaPlot (Systat Software Inc., CA). A P value <0.05 was accepted as statistically significant.

Tissue Usage and Preservation of Organelles. To perform the biochemical experiments, including blue native PAGE and chemical crosslinking, we prepared the mitochondria immediately after completion of the rat experiments. For immune-EM experiments, a small section of the heart tissue was stored in an electron microscopy fixative buffer (15713; Electron Microscopy Sciences, Hatfield, PA). The remainder of the whole heart (about 5–7 g) was snap-frozen in liquid nitrogen and then stored at −80°C. For determining aldosterone synthetic capacity, we determined activity from the mitochondria isolated from the rat heart immediately after completing animal experiments. We compared activity from frozen and fresh tissue but did not find any difference between the two preparations (Acin-Perez et al., 2020). The remaining mitochondria from the tissue sections were not snap-frozen but stored directly at −80°C to avoid membrane rupture due to sudden temperature shock. Fresh mitochondria from the H9c2 cells were isolated as described (Bose et al., 2002; Pawlak et al., 2011; Rajapaksha et al., 2016) immediately after completion of AngII or cAMP stimulation with and without telmisartan and used for in vivo chemical crosslinking experiments.

Transmission Electron Microscopy. Heart tissues were fixed overnight in 4% formaldehyde and 0.2% glutaraldehyde in a 0.1-M sodium cacodylate buffer (pH 7.4), dehydrated through 25%–95% graded ethanol concentrations, and embedded in LR white resin (De Paul et al., 2012). Thin sections (75 nm) were cut with a diamond knife on a Leica EM UC6 ultramicrotome (Leica Microsystems; Bannockburn, IL) and collected on 200 mesh nickel grids. The sections were etched with 2% H_2O_2, quenched with 1 M NH_4Cl, blocked in

Downloaded from jpet.aspetjournals.org at ASPET Journals on April 9, 2024

0.1% BSA in PBS for 4 hours, and then incubated overnight at 4°C with Tom22 antiserum diluted 1:50 in 0.1% BSA. Sections were washed ×5 with PBS and floated on drops of secondary antibody conjugated to ultrasmall (<1.0 nm) NanogoldTM reagent (Nanoprobes, Yaphank, NY) diluted 1:1000 in 0.1% BSA in PBS at room temperature for 2–4 hours. Sections were washed with PBS for 10 minutes five times and with deionized H_2O for 10 minutes five times and then incubated with HQ SilverTM (Nanoprobes) for 8 minutes for silver enhancement, which was followed by washing in cold H_2O to halt the enhancement. For double immunolabeling, the same sections were first labeled with a Tom22 antibody (1:50) overnight at 4°C, which was followed by incubation with antibody to P450c11AS or StAR (1:2000) overnight at 4°C. Silver enhancement for Tom22 was done for twice as long, hence particles corresponding to StAR and Tom22 were of different sizes. To increase the contrast, sections stained with 2% uranyl acetate in 70% ethanol were washed with deionized H_2O for 2 minutes five times and air-dried. The large gold particles averaged 55 nm in diameter (90% were between 45 and 65 nm), and the small gold particles averaged 15 nm with 90% being smaller than 25 nm. Imaging was done with a JEM 1230 transmission electron microscope (JEOL, Peabody, MA) at 110 kV fitted with an UltraScan 4000 CCD camera and Fast Light Digital Camera Controller (Gatan Inc., Pleasanton, CA); 40 sections were analyzed per experiment. Semiquantitative analysis was performed on all grids, with each image divided into 16 quadrants for counting the particles. Each image for each animal was counted five times, and the number of gold particles per field of view is reported ±S.D. with $n = 5$ (for five animals) using Gatan Microscopy Suite software (Gatan Inc.) as described (Prasad et al., 2017).

Mitochondrial Isolation, Purification, and Fractionation. Heart tissues were diced in mitochondrial isolation buffer [250 mM sucrose, 10 mM HEPES, 1 mM EGTA (pH 7.4)]; H9c2 cells were washed with PBS two times, and the mitochondria were isolated as described (Bose et al., 2008). For most experiments, fresh mitochondria were used immediately after their isolation. The mitochondrial compartments were individually purified after a standard procedure with minor modifications (Bose et al., 2008). The purity of the mitochondrial fractions was confirmed by assessing the levels of compartment-specific proteins: cytochrome oxidase complex IV (COX IV) for mitochondrial matrix; VDAC2 and Tom22 for the OMM. We determined mitochondrial viability as described (Prasad et al., 2016); briefly, mitochondrial membrane responsiveness was determined using an ATP Assay System Bioluminescence Detection Kit (ENLITEN; Promega) with a Veritas microplate luminometer (Turner Biosystems, Sunnyvale, CA) following the manufacturer's protocol. ATP production was inhibited by incubating cells with various concentrations of carbonyl cyanide *m*-chlorophenyl hydrazone for 1 hour, as described (Prasad et al., 2017).

Steroid Assays. Arterial blood was obtained from anesthetized rats between 8 and 9 AM by cardiac puncture immediately before sacrifice. Blood was anticoagulated with 0.1 volume of 3.8% sodium citrate, and plasma was separated by centrifugation at 10,000*g* for 20 minutes at 4°C and diluted with PBS at various concentrations to a final volume of 50 μl. Corticosterone was measured by ^{125}I radioimmunoassay (RIA) using a kit (Corticosterone ^{125}I-RIA kit, 07120102) from MP Biomedicals (a division of ThermoFisher, Santa Anna, CA) following the manufacturer's protocol. For plasma steroid values, we compared the control group to the groups with AngII and AngII plus Telmi using ANOVA and Tukey's *t* test of two independent groups corrected for unequal variance.

Aldosterone in culture media from H9c2 cells was also measured by RIA (07108226; MP Biomedicals). Aldosterone synthesis in isolated heart mitochondria was measured by enzymatic conversion of 11-deoxycorticosterone [1,2,3 ^{3}H] (ART 1663; American Radiolabeled Company) as described (Pascoe et al., 1992) using radioactive aldosterone (D-[1,2,6,7-^{3}H(N)]) (NET 814250; Perkin Elmer) as the standard; the assay buffer consisted of mitochondrial import buffer containing 4 μM $MgCl_2$, 0.5 mM NADPH, and 8 mM fumaric acid and NADPH, ferredoxin, and ferredoxin reductase to enhance P450c11AS activity (Psychoyos et al., 1966). Heart mitochondria were pooled from three animals from each group, yielding ~100 μg total protein per ml of assay buffer, and the assays were done five times from three separate pools of mitochondria. Steroid conversion was then assessed by thin-layer chromatography.

Native Immunoblot Analysis. Mitochondria were isolated from heart tissues or from H9c2 cells as described (Bose et al., 2008); native complexes were isolated by incubating the mitochondria in buffer containing 1% digitonin, and samples were separated by electrophoresis through 3%–16% or 4%–20% native gradient gels. After the protein complexes were transferred to a polyvinylidine difluoride membrane, they were blocked with 3% nonfat dry milk for 45 minutes, probed overnight with the primary antibodies, and then incubated with peroxidase-conjugated goat anti-rabbit IgG or anti mouse IgG (Pierce, Rockford, IL). Signals were developed with a chemiluminescent reagent (Pierce). For direct visualization of the complexes, the gels were stained with Serva blue or Coomassie Blue overnight at 4°C. Unless otherwise indicated, antibodies to P450c11AS (Adams and Bose, 2012), VDAC2 (Prasad et al., 2015), and StAR (Bose et al., 1999) were purchased from Santa Cruz Biotechnology (Santa Cruz Biotech) or AbCam (Boston, MA).

Two-Dimensional and Native Gradient PAGE. For 2D native PAGE, first one-dimensional native PAGE was run, the complex was excised, and a second native PAGE was performed in the perpendicular direction. For analysis of proteins in the large complexes detected by native Western blotting, mitochondria were reisolated by washing with import buffer followed by centrifugation, then lysed in 1% digitonin, 20 mM Tris-HCl (pH 7.4), 0.1 mM EDTA, 50 mM NaCl, 10% glycerol, and 1 mM phenylmethylsulfonyl fluoride for 15 minutes on ice. The digitonin lysate was combined with native PAGE sample buffer [5% Coomassie Brilliant Blue G-250, 100 mM 2-[bis(2-hydroxyethyl)amino]-2-(hydroxymethyl)propane-1,3-diol (pH 7.0), 500 mM 6-aminocaproic acid] and subjected to 3%–16% gradient native PAGE at 100 V overnight at 4°C. Protein complexes were further fractionated by applying 100 μl of digitonin lysate to a 30%–10% sucrose step gradient with a 200-μl 66% sucrose cushion at the bottom (final volume, 2.0 ml). After centrifugation at 55,000*g* in a Beckman TLA55 rotor for 4 hours, the sample was immediately equally aliquoted and loaded onto gradient, native PAGE, or SDS-PAGE gels. Radiolabeled proteins were detected by autoradiography or on a PhosphorImager.

Mass Spectrometry. Bands from native gradient PAGE that were identified with a specific antibody, Serva blue, or Coomassie Blue were excised, reduced with dithiothreitol (Roche, Pleasanton, CA), alkylated with iodo-acetamide (Sigma), and subjected to in-gel digestion with trypsin (trypsin gold, sequencing grade; Promega). Sample cleanup was completed with Millipore C18 ZIPTips (Billerica, MA) on the extracted peptides prior to drying and resuspension in 0.1% formic acid in water. Each sample was then analyzed by UHPLC-MS/MS on a Waters nanoAcquity UHPLC(Ultra High Performance Liquid Chromatography)coupled to a Waters Q-TOF Premier (Waters, Milford, MA) as described (Swartz, 1991). A 5-μl injection was made onto a ThermoFisher 0.3 mm ID × 1 mm C18 PepMap nanoTrap cartridge equipped with nanoViper fittings. After trap cartridge washing with 99% water containing formic acid (1% acetonitrile), the peptides were separated on a ThermoFisher Acclaim C18 PepMap 100 with dimensions of 75 μm × 15 cm, 3 μm with 100-Å pore. Peptides were separated using a water/acetonitrile gradient containing 0.1% formic acid from 1% to 60% acetonitrile in 45 minutes. Liquid chromatography followed by mass spectrometric analysis (LC-MS/MS) raw data sets were extracted using Mascot Distiller and subjected to data base searching using a Mascot MS/MS ion search to identify proteins considering oxidation of methionine and alkylation of cysteine (Rosenfeld et al., 1992).

In Vitro Protein Crosslinking and Coimmunoprecipitation Analysis. Heart mitochondrial fractions were incubated with 0, 0.5, 1.0, 2.0, or 5.0 mM bis(sulfosuccinimidyl)suberate (BS^3) (Thermo Fisher) solubilized in PBS. After 1 hour, the crosslinking was

Downloaded from jpet.aspetjournals.org at ASPET Journals on April 9, 2024

terminated by transferring the samples to ice and adding 10 μl of 1.0 M Tris buffer, pH 9.0. The crosslinked fractions were collected by centrifugation at 3000 rpm, (Allegra 22XR; Beckman centrifuge fitted with a 2240 rotor) and lysed with 1% digitonin (Bose et al., 2008). Mitochondrial pellets were resuspended, washed, clarified by ultracentrifugation, and incubated with antibodies to IgG, COX IV, StAR, P450c11AS, or Tom22 prebound to protein A-Sepharose beads. Specific antibodies were preincubated with protein A-Sepharose CL 4B (0.5 μg/μl; Amersham Biosciences, Sweden) in 100 μl of coimmunoprecipitation (co-IP) buffer (1% Triton X-100, 200 mM NaCl, and 0.5% sodium deoxycholate) and mixed on an end-over-end rotator for 2 hours at 4°C. To remove unbound antibody, the Sepharose beads were washed with co-IP buffer five times and then incubated again with purified rat IgG control antibody (Sigma) for 1 hour to block unbound protein A. After another series of washes to remove unbound antibody, the freshly isolated mitochondrial pellet (25 mg protein for each sample) was resuspended with ice-cold lysis buffer [20 mM Tris-HCl (pH 8.0), 137 mM NaCl, 10% glycerol, 1% Triton X-100, 2 mM EDTA] and incubated at 4°C for 15 minutes. Insoluble material was removed by ultracentrifugation (30 minutes at 100,000*g*). The supernatants were incubated overnight at 4°C with shaking in the presence of antibodies prebound to protein A-Sepharose beads. After five to six washes with 1× co-IP buffer and two washes with 10 mM HEPES (pH 7.4), the protein A-Sepharose pellets were resuspended and vortexed with 100 mM glycine (pH 3.0) for 10 seconds. The sample was adjusted to pH 7.4 by adding a pretitrated volume of 1.0 M Tris (pH 9.5), and the beads were separated from the soluble material by centrifugation at 2000*g* for 2 minutes. The supernatants (immune complexes) were analyzed by immunoblotting with P450c11AS, Tom22, or StAR antibodies.

Figure Preparation and Data Analysis. Images were obtained from autoradiographic films or scanning with a PhosphorImager, and the data were analyzed using Kalidagraph or Microsoft Excel and reported as mean ± S.E. To compare quantitated images, we used one-way ANOVA and the Welch *t* test of two independent groups (Welch, 1947) corrected for unequal variance to analyze group differences. We conducted both two-sided and one-sided Welch *t* tests. For all statistical analyses, we also conducted a Tukey's honest significant difference test based on one-way ANOVA, a Kruskal-Willis test, and one-way ANOVA comparison of the three groups. Welch's *t* test was ultimately chosen and concurs with *P* values from all other statistical analyses conducted. The *P* values generated from each set of statistical tests were all statistically significant ($P < 0.05$) and very similar; the highest of the *P* values are reported.

Results

Aldosterone Synthesis in the Rat Heart. Because cardiac biosynthesis of aldosterone has been questioned (Ye et al., 2005; MacKenzie et al., 2012), we studied cardiac steroidogenesis in rats receiving AngII continuously infused by minipumps for 2 or 4 weeks, at which point cardiac fibrosis developed. We also challenged AngII action by daily intragastric administration of telmisartan, which inhibits the interaction of AngII with its receptor and does not alter the activity of most cytochrome P450 enzymes (Schupp and Unger, 2005); these animals were compared with controls receiving saline via minipumps. In other experiments (Zhang et al., 2020), serum aldosterone in control rats was 0.8 ng/ml (2.2 nM), 4 weeks of AngII infusion raised this to 7.1 ng/ml (19.7 nM), and 4 weeks of AngII plus telmisartan yielded 1.1–1.3 ng/ml (3.1–3.6 nM) aldosterone, showing nearly complete blockade of the action of AngII. AngII infusion increased serum corticosterone about 350-fold, from 10.7 ± 1.8 (S.D.) ng/ml (29 ± 4.9 nM) in control (sham) animals to

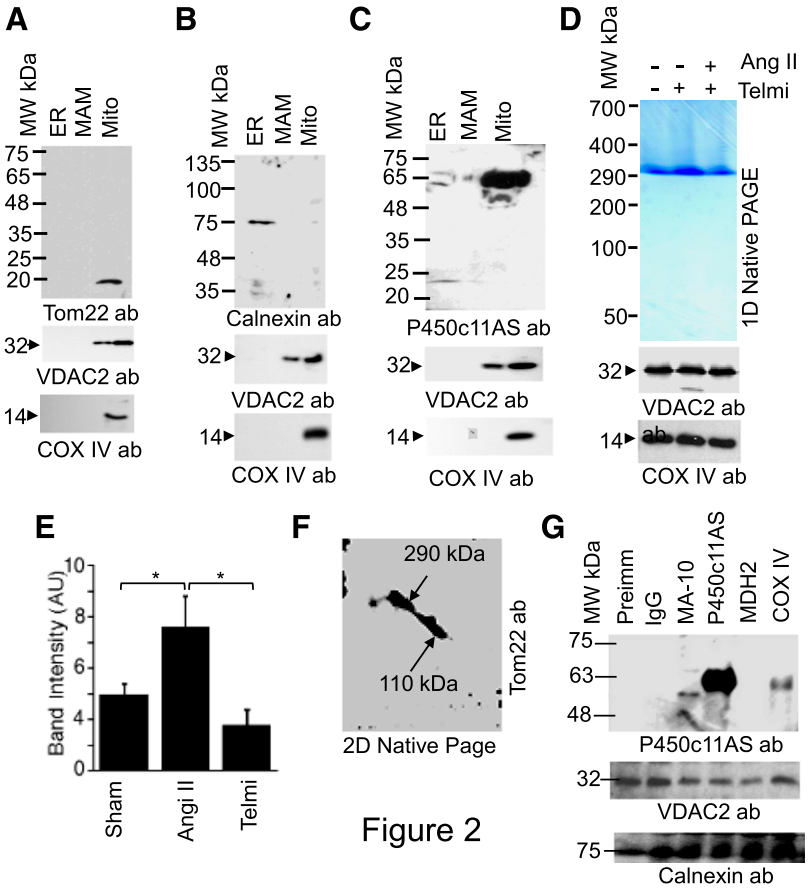

Figure 2

Fig. 2. Heart mitochondrial complex. (A–C) Proteins from rat heart ER, MAM, and mitochondria (Mito) were immunoblotted with antibodies to Tom22 (A), calnexin (B), P450c11AS (C) (top panels), VDAC2 (middle), and COX IV (bottom), confirming the accuracy of organelle fractionation. (D) Coomassie Blue–stained native gradient PAGE of digitonin-solubilized heart mitochondria from untreated animals, animals receiving AngII for 4 weeks (AngII), and animals receiving AngII and telmisartan. Bottom panels: immunoblots showing equivalent protein loading in the blue native PAGE. (E) Estimation of the amount of protein present in the 290-kDa band from scanning of five gels of the type shown in (D). Comparisons designated by an asterisk (*) had *P* values <0.05. (F) 2D native gradient PAGE of the 290-kDa band from (D) blotted with anti-Tom22. (G) Coimmunoprecipitation of the digitonin lysate of the 290-kDa complex with the indicated antibodies displayed by PAGE and blotted with antisera to P450c11AS; middle panel: blotting of the same membrane with anti-VDAC2; bottom panel: immunoblot of the same SDS-PAGE with antiserum to calnexin. MW, molecular mass.

Downloaded from jpet.aspetjournals.org at ASPET Journals on April 9, 2024

TABLE 1
Mass spectrometric analyses of complexes isolated from sham-operated hearts
1. Mitochondrial complex 290-kDa from one-dimensional native PAGE from control, sham-operated hearts

Accession No.	Protein	MS/MS Score	No. of Unique Peptides
153791547	ATP synthase-β mitochondrial	802	17
3939	Lactate dehydrogenase	702	13
176644268	Heat shock protein	318	5
2506849	Malate dehydrogenase	213	4
113205888	Aldehyde dehydrogenase	141	2
2168	Fatty acid binding protein	129	3
25557	StAR	98	3
56993	Tom22	98	2
19961	COX IV	81	3
129378	P450c11AS	69	4

3.7 ± 0.25 μg/ml (11 ± 0.75 μM) ($P < 0.0005$) in those receiving AngII, which was reduced dramatically (41.4 ± 0.17 ng/ml; ~120 nM) by cotreatment with telmisartan. Because studies directly examining aldosterone in cardiac tissue are complicated by cardiac uptake of circulating aldosterone, we directly assayed aldosterone biosynthetic capacity in isolated mitochondria. Left ventricles were removed, washed, weighed, and homogenized, and mitochondria were prepared, incubated with DOC, and assayed for aldosterone synthesis (Fig. 1B). Mitochondria from control hearts produced ~24 μg of aldosterone per gram of heart tissue; 2 weeks of AngII infusion did not change this aldosterone synthesis, but it was reduced to barely detectable by treatment with telmisartan. Hearts from rats receiving AngII for 4 weeks produced more aldosterone than did the hearts of control (sham) animals (53 vs. 24 μg per gram of heart tissue) ($P \leq 0.001$), and telmisartan treatment reduced aldosterone production to below that seen in control animals (24 vs. 13 μg/g) ($P \leq 0.001$) (Fig. 1B). Expression of voltage-dependent access channel 2 (VDAC2), a protein in the OMM, and the expression of COX IV, a mitochondrial matrix protein, remained unchanged (Fig. 1B, bottom panels), indicating that other mitochondrial proteins were not affected and confirming that each lane received equal amounts of protein. Because 4 weeks of AngII induced a greater production of aldosterone (Fig. 1B) and because 4 weeks of AngII was required to produce clear cardiac fibrosis (Fig. 1C), all subsequent animal experiments were done with 4 weeks treatment.

Cardiac Fibrosis Induced by AngII. An experimental period of 4 weeks was selected based on induction of cardiac fibrosis with AngII infusion. The fibrotic area with collagen deposition was identified by Masson's trichrome staining (Fig. 1C). Quantitation of this fibrotic area from slides from each experimental animal showed approximately a 70fold increase with 4 weeks of AngII infusion (Fig. 1D, $P < 0.001$ vs. sham), which was significantly reduced by cotreatment with telmisartan (Fig. 1D, $P < 0.001$ vs. AngII). AngII increased the number of mitochondria per cell, and telmisartan reduced mitochondrial counts to below control values (Fig. 1E); this may reflect a trophic as well as tropic action of AngII in the heart. Transmission EM suggested that mitochondria in AngII-treated hearts were not distributed uniformly but accumulated in local regions; telmisartan reduced mitochondrial number and size compared with the untreated mitochondria. AngII also appeared to alter the structure of the cristae, and this was reversed by telmisartan. Thus, AngII via the AT1 receptor altered mitochondrial morphology and cellular distribution. Coincidently, with reduced cardiac fibrosis, the ratio of heart weight to body weight in the animals treated with telmisartan was significantly reduced compared with that of the untreated mitochondria.

A Heart Mitochondrial Complex of P450c11AS, StAR, and Tom22. Aldosterone synthesis requires P450c11AS, which is associated with the IMM and converts DOC to aldosterone. Detecting aldosterone synthesis in rat heart mitochondria implied that these mitochondria should contain P450c11AS. We prepared IMM containing the respiratory chain complex, solubilized it with digitonin, and separated the proteins by gradient blue native PAGE. Immunoblotting confirmed the accuracy of the mitochondrial preparation and fractionation. Mitochondria contain Tom22 (a component of the mitochondrial protein import machinery) and COX IV but lack calnexin, whereas ER contains calnexin but not Tom22 or COX IV (Fig. 2, A and B). VDAC2, an OMM protein facing the cytoplasm, is part of the mitochondria-associated membrane (MAM) (Naghdi et al., 2015; Naghdi and Hajnóczky, 2016); thus, finding VDAC2 in the MAM is the expected result (Fig. 2, B and C). A major complex of 290 kDa was apparent (Fig. 2D), increased in intensity 1.7-fold with AngII ($P = 2 \times 10^{-4}$ n = five experiments), and decreased by 50% with telmisartan cotreatment [$P > 0.05$], suggesting this complex may contain P450c11AS (Fig. 2E). LC-MS/MS detected several proteins in the 290-kDa complex, including P450c11AS, StAR, and the mitochondrial translocase Tom22 (Table 1-3). Thus, the mitochondria from rat heart stimulated with AngII contain P450c11AS, and P450c11AS may require an association with Tom22 and StAR.

Two-dimensional native PAGE identified components of the 290-kDa complex. Immunoblotting with anti-Tom22

TABLE 2
Two hundred ninety–kilodalton complex from 2D native gradient PAGE

Accession No.	Protein	MS/MS	No. of Unique Peptides
113205888	Malate dehydrogenase	190	2
2168	Aldehyde dehydrogenase	171	2
56993	StAR	105	1
19961	Tom22	105	2
129378	P450c11AS	94	1

Downloaded from jpet.aspetjournals.org at ASPET Journals on April 9, 2024

TABLE 3
One hundred ten–kilodalton complex from 2D native gradient PAGE

Accession No.	Protein	MS/MS	No. of Unique Peptides
56993	StAR	105	1
19961	Tom22	105	2
129378	P450c11AS	124	3

identified complexes of 290 kDa and 110 kDa (Fig. 2F); LC-MS/MS showed the 110-kDa complex contained only Tom22, StAR, and P450c11AS (Table 3), whereas the 290-kDa complex contained these and other proteins (Table 1-3). COX IV and aldehyde dehydrogenase do not affect mitochondrial protein import (Rajapaksha et al., 2013), and coimmunoprecipitation showed that malate dehydrogenase did not interact with P450c11AS (Fig. 2G). Immunoblotting with antiserum to calnexin showed that equivalent amounts of protein were applied in each lane (Fig. 2G, bottom panel). The LC-MS/MS analyses were done 3 to 4 times, but P450scc was never detected in these complexes, indicating that the heart lacks the capacity to initiate steroidogenesis from cholesterol.

Localization and Quantitation of P450c11AS, StAR, and Tom22. Immunocytochemistry located P450c11AS, StAR, and Tom22 in the perivascular region and inner myocardium in control hearts (Fig. 3A). StAR was constitutively expressed in the tunica intima (vessel endothelium) and the tunica media (concentrically arranged smooth muscle cells), whereas P450c11AS and Tom22 were detected in the tunica media. AngII increased while telmisartan markedly attenuated the diffuse, cytoplasmic signals for P450c11AS, StAR, and Tom22 expressed in the arterioles and intermyocardium (Fig. 3A). After AngII, the number of intracardiac vessels containing P450c11AS, StAR, and Tom22 was 2.4 ± 1.0, 2.4 ± 0.4 and 2.2 ± 0.7/HPF High-Power Field), respectively; telmisartan reduced this to 0.4 ± 0.1, 0.6 ± 0.4 and 0.8 ± 0.6/HPF, respectively (all $P < 0.05$) (Fig. 3A). Thus, AngII increased StAR expression, and telmisartan may have prevented complex formation because of limited expression of StAR.

Immunogold transmission electron microscopy (TEM) was consistent with the immunohistochemistry. Mitochondria in control hearts contained small amounts of StAR. AngII increased the abundance of StAR and increased collagen, myosin, and actin filaments (indicating fibrosis); telmisartan reduced StAR expression in AngII-treated animals. Control hearts contained P450c11AS; AngII increased and telmisartan reduced P450c11AS compared with controls. Tom22 was minimally expressed in control hearts, AngII increased its expression slightly, and coadministration of telmisartan inhibited Tom22. Independent labeling with antibodies to P450c11AS and Tom22 showed that P450c11AS was abundantly expressed, but Tom22 levels were low (Fig. 3B). Similar analysis with P450c11AS and StAR showed that StAR increased with AngII infusion. The TEM data were quantitated by counting the immunogold particles in 40 images from each experimental group (Fig. 3B). In controls, there were 7 ± 1.6 StAR-labeled particles per field of view (81 μm^2); AngII increased StAR to 22 ± 3 particles/field ($P = 0.0014$), and telmisartan reduced this increase to 4 ± 0.7/field ($P = 0.0031$) (Fig. 3B, left). In controls, P450c11AS was present at 6.5 ± 0.2/field and was essentially unchanged with AngII (7.2 ± 0.3/field) or with telmisartan (6.2 ± 0.1/field) (Fig. 3B). Similarly, AngII slightly increased Tom22 from 1.65 ± 0.1 to 3.0 ± 0.21/field ($P = 0.0025$), which decreased to basal with telmisartan (1.3 ± 0.07/field) (Fig. 3B, right) ($P = 0.0087$).

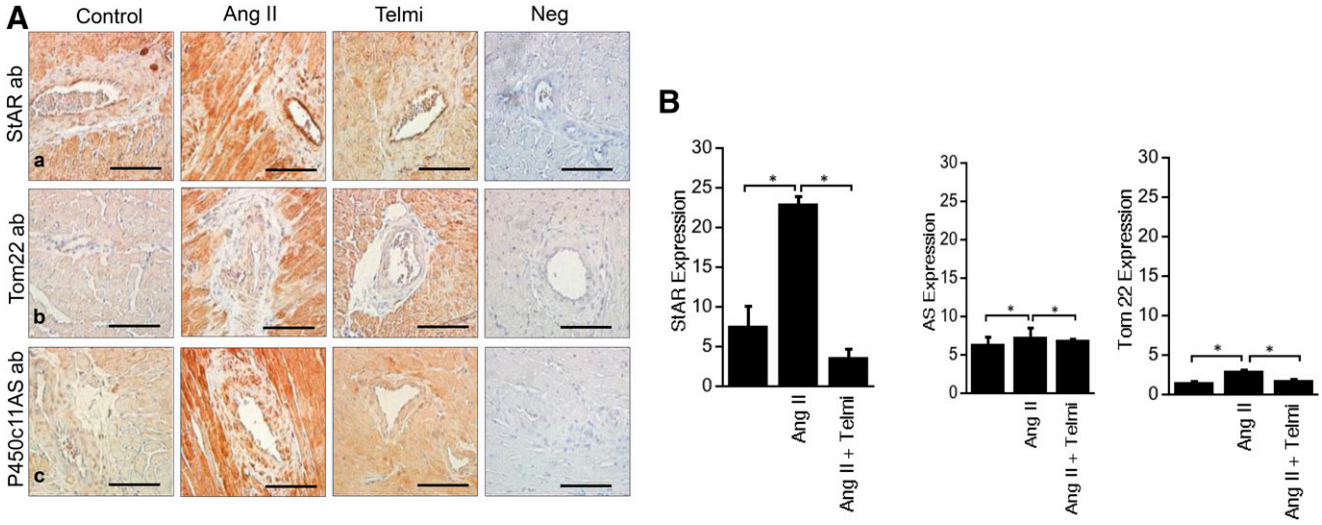

Fig. 3. Immunocytochemistry. (A) Representative images of heart tissue stained with antisera to StAR, Tom22, and P450c11AS. Cardiac tissue from animals in the three treatment groups (designated above figure) was stained with antisera (designated at left). StAR, Tom22, and P450c11AS (AS) were markedly increased in intracardiac vessels and intermyocardium after 4 weeks of AngII, which was markedly inhibited by telmisartan; no staining was seen without the primary antibodies (Neg); original magnification: 400×; scale bars, 100 μm. (B) Quantitation of StAR (left panel), P450c11AS (middle panel), and Tom22 (right panel) from TEM. Data are mean ± S.E.M. of three experiments, each performed in triplicate. *P* values designated by an asterisk (*) are <0.05.

Downloaded from jpet.aspetjournals.org at ASPET Journals on April 9, 2024

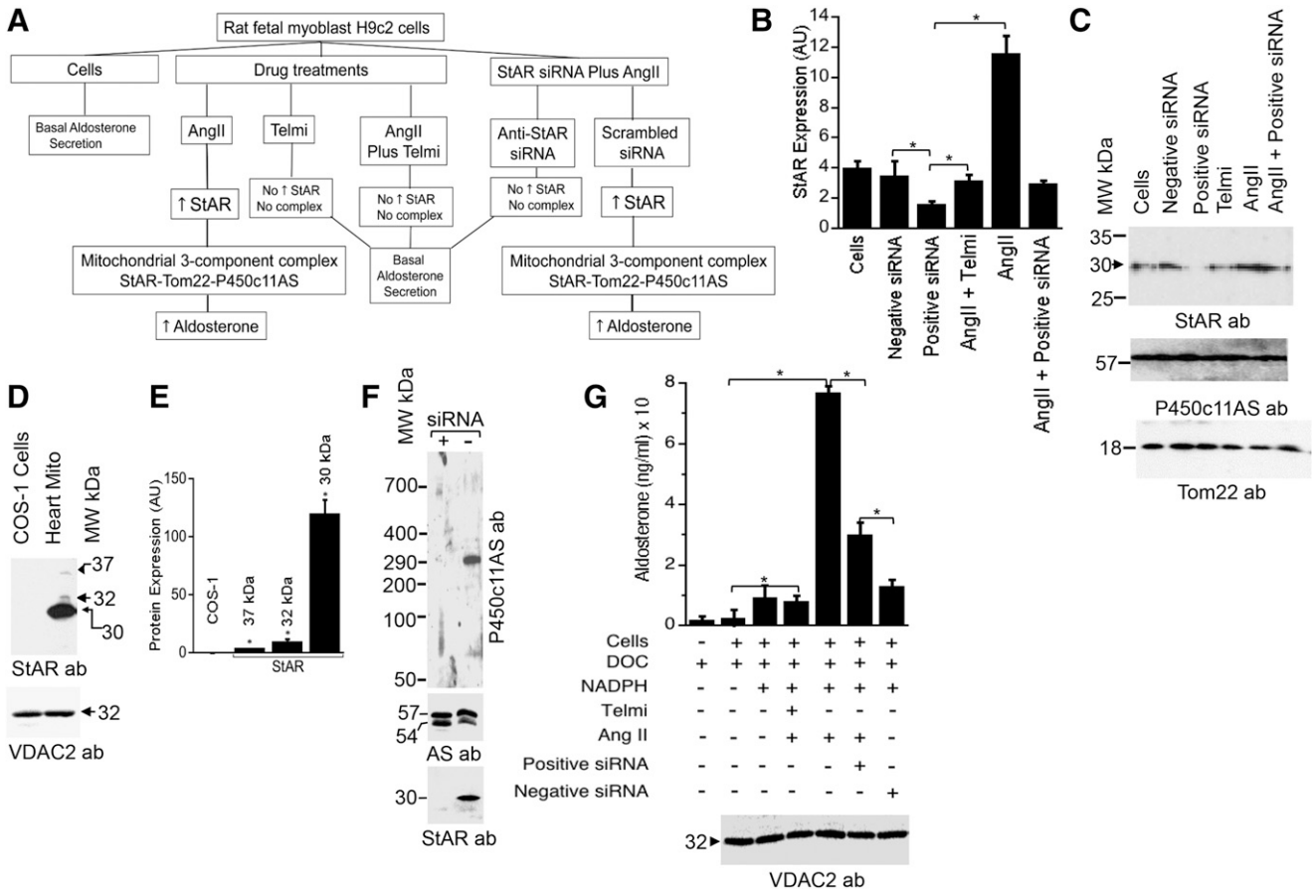

Fig. 4. Role of StAR in P450c11AS expression. (A) Flow diagram for experiments with rat fetal myoblast H9c2 cells. Control cells secreted low but measurable levels of aldosterone. Treatment with AngII alone promoted expression of StAR and formation of the StAR-Tom22-P450c11AS complex and increased aldosterone secretion; the same result was seen in cells receiving AngII plus control, scrambled-sequence siRNA (far right). Treating cells with telmisartan alone, with AngII plus telmisartan, or with siRNA directed against StAR reduced aldosterone secretion to or nearly to basal levels. (B) Quantitation of densitometric scanning of PAGE of H9c2 cell extracts blotted with anti-StAR. Cells were incubated with (left to right) no additive, negative (scrambled) siRNA (Negative siRNA), siRNA against StAR (Positive siRNA), AngII + telmisartan, AngII, and AngII plus + Positive siRNA against StAR. AngII increased StAR expression, which was reduced to control values by telmisartan or anti-StAR siRNA. The experiment was done three times, and the densitometric scanning data (reported as arbitrary units, AU) are reported as mean ± S.E.M.; * designates $P < 0.05$. (C) Expression of StAR, P450c11AS, and Tom22 in H9c2 cells alone or after incubation with negative (nonspecific sequence) siRNA (−ve siRNA), StAR knockdown by siRNA (Positive siRNA), incubation with telmisartan (Telmi), incubation with AngII, and incubation with AngII plus anti-StAR siRNA. The blot was sequentially probed with anti-StAR (top), anti-P450c11AS (middle), and anti-Tom22 (bottom). (D) Representative gel showing processing of StAR in heart mitochondria (top) and immunoblotting for VDAC2 indicating equivalent protein loading (bottom). (E) Quantitation of StAR from three gels, as shown in (D). (F) Native gradient PAGE of proteins from H9c2 cells treated without (minus sign) or with (plus sign) siRNA directed against StAR and blotted with anti-P450c11AS. Bottom panels show SDS-PAGE followed by blotting with antibodies to P450c11AS (AS) or StAR. (G) Aldosterone synthesis by H9c2 cells (ng/ml of culture medium after 24 hours) incubated with various combinations of DOC, NADPH, Telmi, AngII, siRNA against StAR (siRNA), and control, scrambled-sequence (negative) siRNA (−ve siRNA); treatments are indicated by "+" (added) or "−" (omitted). Bottom panel, VDAC2 immunoblotting from these H9c2 cells. Bars 1 and 2 (from left) show that added DOC did not influence the aldosterone assay. Bars 3 and 4: Adding NADPH permitted some aldosterone synthesis, which was unchanged by AngII + telmisartan or by control, −ve siRNA (bar 7). Bar 5: AngII increased aldosterone production ~6-fold, which was reduced by siRNA against StAR (bar 6). The experiment was performed three times, and P values were all <0.02. MW, molecular mass.

P450c11AS Activity in Heart Requires StAR. AngII increased cardiac aldosterone synthetic capacity (Fig. 1B), but there was minimal change in P450c11AS (Fig. 3B, middle), indicating additional factors besides P450c11AS are involved in cardiac aldosterone synthesis. AngII increased and telmisartan inhibited StAR expression in rat heart (Fig. 3B, left), and the exposed C-terminal regions of Tom22 and P450c11AS interacted in the mitochondrial IMS (Intermembrane space) (Prasad et al., 2016). Thus, we hypothesized that interaction of P450c11AS with Tom22 is facilitated by 30-kDa StAR, even though no role for intramitochondrial 30-kDa StAR has been established and no role for StAR in P450c11AS activity has been proposed.

To explore StAR's potential action on P450c11AS, we used rat fetal myoblast H9c2 cells (Fig. 4A). These cells express P450c11AS and StAR, which was induced by AngII and inhibited by telmisartan (Fig. 4, B and C). Knockdown of StAR in AngII-stimulated H9c2 cells with siRNA against StAR (positive siRNA) reduced its expression by nearly 80% (Fig. 4B, last lane) without affecting expression of Tom22 and P450c11AS (Fig. 4C), similar to results in rat heart (Fig. 3B). Thus, StAR appears to play an important role in cardiac aldosterone synthesis. When promoting adrenal or gonadal steroidogenesis, StAR is active on the OMM as its 37-kDa primary transcript (sometimes termed a "precursor") (Bose et al., 2002). However, more than 95% of StAR present in heart mitochondria is the processed, intramitochondrial 30-kDa form, which is inactive in promoting cholesterol influx (Bose et al., 2002), and there were

Downloaded from jpet.aspetjournals.org at ASPET Journals on April 9, 2024

negligible amounts of the 37- and 32-kDa forms (Fig. 4, D and E). This suggests that 30-kDa StAR is the active form in the heart. StAR knockdown inhibited formation of the 290-kDa P450c11AS complex, even though expression of P450c11AS was unchanged (Fig. 4F). Thus, the expression of P450c11AS is independent of StAR and Tom22, and StAR appears to interact with P450c11AS without affecting its expression. StAR knockdown inhibited aldosterone synthesis from DOC added to H9c2 cells (Fig. 4G). The left-most two bars show that DOC did not crossreact in the aldosterone assay, but addition of DOC and NADPH (needed by P450c11AS) resulted in 13 ± 1.4 ng/ml aldosterone (P = 0.0015) (third bar), which was not affected by AngII plus telmisartan (P = 0.967) (fourth bar). AngII treatment without telmisatan increased aldosterone from 13 ± 1.4 to 77 ± 2.0 ng/ml (P = 0.0019) (fifth bar), but knockdown of StAR reduced this AngII-induced value to 30.9 ± 4.1 ng/ml (P = 0.0041) (sixth bar). In the absence of AngII, the aldosterone produced by cells treated with control, negative siRNA (seventh bar) was not different from the control (third bar) (Fig. 4G). Immunoblotting with anti-VDAC2 confirmed that equivalent amounts of mitochondrial proteins were applied in each lane (Fig. 4G). Thus aldosterone production by P450c11AS in H9c2 cells requires StAR, suggesting that this mechanism also applies to the intact heart.

P450c11AS Interacts with StAR through Tom22. The 290-kDa and 110-kDa mitochondrial complexes contained P450c11AS, StAR, and Tom22 (Table 1-3), but how these proteins interact was unknown. The predominant form of StAR in heart tissue is the intramitochondrial 30-kDa form (Fig. 4, D and E), whereas P450c11AS was present as both the 57-kDa precursor and 54-kDa intramitochondrial forms (Fig. 5A) with similar abundances (Fig. 5B); this gross excess of 30-kDa StAR suggests it may be the form interacting with P450c11AS. To explore the potential association of P450c11AS with StAR and Tom22, we solubilized heart mitochondria with digitonin, fractionated the products on density gradients, and examined the fractions with antibodies to P450c11AS, Tom22, and StAR. There was some overlap of P450c11AS with Tom22 in fractions 5–7 (Fig. 5, C and D), substantial overlap of P450c11AS and StAR in fractions 7–11 (Fig. 5, E and F), and nearly complete overlap between Tom22 and StAR in fractions 4–9 (Fig. 5, G and H). This partial overlap suggests protein-protein interactions, as confirmed below in Fig. 6. The separation between the proteins demonstrates that these interactions are not covalent, but the overlap indicates they are fairly tightly associated with one another, and thus even our 4-hour density gradient separation could not achieve full separation despite the differences in the molecular sizes of the proteins. The association was greatest between Tom22 and StAR (Fig. 5, G and H), confirming that the imported StAR remained associated with Tom22. Thus, P450c11AS interacted with StAR to a greater extent than with Tom22.

P450c11AS Must Interact with StAR for Aldosterone Synthesis in Rat Heart. Stimulating H9c2 cells with either cAMP or AngII increased StAR expression 2.5-fold without affecting expression of VDAC2 or P450c11AS (Fig. 6A). There was minimal difference in the expression of Tom22 when H9c2 cells were treated with AngII, but Tom22 expression decreased with telmisartan (Fig. 6B), suggesting that telmisartan, by interfering with the action of AngII, reduces the interaction between StAR and Tom22. Coimmunoprecipitation experiments showed that compared with untreated cells AngII increased and telmisartan reduced the interaction between StAR and P450c11AS (Fig. 6C). StAR, Tom22, and P450c11AS were also coimmunoprecipitated with each other's antibody (Fig. 6, D and E), suggesting that Tom22 plays a role in the interaction between StAR and P450c11AS. Immunoblotting before the coimmunoprecipitation showed equivalent

Downloaded from jpet.aspetjournals.org at ASPET Journals on April 9, 2024

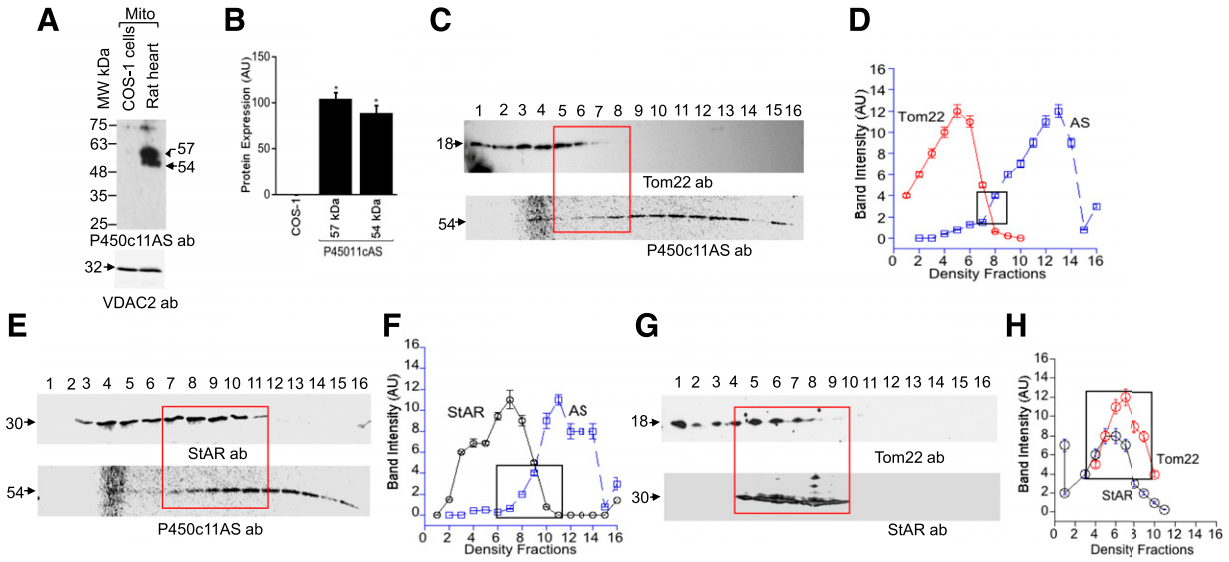

Fig. 5. Interaction of StAR and P450c11AS. (A) Immunoblotting identifies 57- and 54-kDa P450c11AS in heart mitochondrial cells but not in COS-1 cells. Bottom panel: Probing with anti-VDAC2 confirms equivalent protein loading in each lane. (B) Quantitation of the data in (A); the difference in the amounts of 57- and 54-kDa P450c1AS is not significant. (C) Immunoblots of density gradient fractions of heart mitochondria using anti-Tom22 and anti-P450c11AS (AS). (D) Quantitation of the data from (C). (E) Immunoblots of density gradient fractions of heart mitochondria using anti-StAR and anti-P450c11AS. (F) Quantitation of the data from (C). (G) Immunoblots of density gradient fractions of heart mitochondria using anti-Tom22 and anti-StAR. (H) Quantitation of the data from (G). The overlapping distribution is highlighted by a red square in (C, E, and G) and by a black square in (D, F, and H). Data in (B, D, F, and H) are mean ± S.E.M. of three independent experiments, each performed in triplicate. AU, arbitrary unit; Mito, mitochondria; MW, molecular mass.

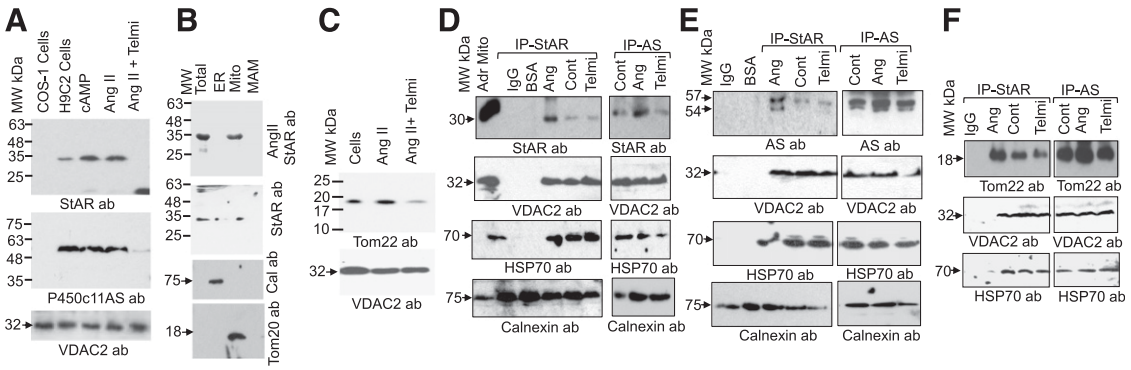

Fig. 6. Interaction of P450c11AS with Tom22 and StAR. (A) Immunoblot of H9c2 proteins with anti-StAR (top), anti-P450c11AS (middle), and anti-VDAC2 (bottom, protein loading control). COS-1 cells (first lane) do not express StAR (negative control); the other lanes contain H9c2 cell proteins, untreated or incubated with cAMP, AngII, or AngII + telmisartan. (B) Distribution of StAR in the mitochondria (Mito), in the MAM, and in the ER, isolated from AngII-treated animals (top) or untreated animals (second from top); the gels were immunostained with StAR antibody. The bottom two panels show the accuracy of the cellular fractionation by immunoblotting for calnexin (Cal) (specific for the ER) and Tom22 (specific for the OMM). (C) Tom22 expression in H9c2 cells, untreated or incubated with AngII or AngII + telmisartan. Bottom panel: blotting with anti-VDAC2. (C–E) Coimmunoprecipitation experiments. (D) Proteins from untreated H9c2 cells [control (Cont)] or treated with AngII (Ang) or AngII + telmisartan (Telmi) were immunoprecipitated with anti-StAR (IP-StAR) or anti-P450c11AS (IP-AS) followed by immunoblotting with anti-StAR, anti-VDAC2, or anti-HSP70. (E and F) Coimmunoprecipitation as in (C) probed with anti-P450c11AS (D) or anti-Tom22 (E); in (E), the control (Cont) is untreated rat heart. Bottom panels: independent immunoblotting with anti-VDAC2, anti-HSP70, and anti-calnexin antibodies. AS, P450c11AS; MW, molecular mass.

amounts of VDAC2 and HSP70, confirming equivalent sample loading in each lane; this was also confirmed by immunoblotting for calnexin (Fig. 6, C and D).

Three-Component Interaction during Processing at the IMS. To understand how Tom22, StAR, and P450c11AS interact, we performed in vitro chemical crosslinking with BS^3 in rat heart mitochondria. After crosslinking, the native 57-kDa P450c11AS band, 18-kDa Tom22 band, and 30-kDa StAR band (Fig. 7, A–C, left panels) that were seen without BS^3 disappeared, and new bands of 85-kDa and 110-kDa were seen with increasing BS^3 concentrations, suggesting that P450c11AS, Tom22, and StAR had become crosslinked to one another. Crosslinking was optimal at 2 mM, but 5 mM BS^3 generated nonspecific protein aggregation. Coimmunoprecipitation of the 2 mM crosslinked products followed by immunoblotting with antisera to P450c11AS, Tom22, and StAR confirmed the specificity of interactions of Tom22, P450c11AS, and StAR, as only the 110-kDa product (crosslinking of 57-kDa P450c11AS, 18-kDa Tom22, and 30-kDa StAR) was seen with each antibody (Fig. 7, A–C right panels). Immunoblotting the crosslinked products with antiserum to COX IV only identified COX IV itself, showing that the treatment with BS^3 did not crosslink other, unassociated mitochondrial proteins (Fig. 7, A–E right hand bottom panels). Equivalent immunodetectable VDAC2 was seen in each lane, confirming equal sample loading.

We confirmed the intracellular interaction of P450c11AS, StAR, and Tom22 by in vivo crosslinking in H9c2 cells; 2 mM BS^3 again gave optimal results. Immunoblotting with anti-P450c11AS showed a 110-kDa band that increased in intensity with increasing BS^3 concentrations (Fig. 7, D and E) and decreased with siRNA knockdown of StAR (Supplemental Fig. 1, A and C; Supplemental Fig. 2, A and C). As with the crosslinking in heart mitochondria, this 110-kDa band represents the interaction of P450c11AS, StAR, and Tom22. The intensity of the 110-kDa band was not affected by AngII (Supplemental Figs. 1 and 2) or siRNA against StAR, possibly because of the limited increase in P450c11AS. Immunoblotting with antiserum to COX IV did not identify any proteins other than COX IV, confirming the specificity of the co-IP experiment (Fig. 7, D and E, right hand bottom panels). Thus the interaction of P450c11AS with Tom22 and 30-kDa StAR is seen in both heart and H9c2 cells.

Discussion

In unstressed rats, others have reported that the amount of immunoassayable intracardiac aldosterone corresponded to circulating concentrations, and P450c11AS mRNA was not found, thus bringing into question intracardiac aldosterone synthesis (Gomez-Sanchez et al., 2014). Another study found P450c11AS in the rat heart and in the fetal human heart but not in the adult human heart (Kayes-Wandover and White, 2000). However, those authors cautioned that P450c11AS might be produced in the human heart during sodium depletion, heart failure, or myocardial infarction (i.e., during stress). These studies have resulted in the general view that cardiac aldosterone synthesis or P450c11AS are unlikely to be found in physiologically significant amounts (MacKenzie et al., 2012). We have modeled cardiac stress in rats by infusing AngII to the point of generating cardiac fibrosis, clearly showing that these conditions induce the synthesis of aldosterone and expression of P450c11AS in the rat heart.

StAR is abundantly expressed in infarcted mouse left ventricular fibroblasts 3 days after ligating the left anterior descending coronary artery, but expression in myocytes was not reported (Anuka et al., 2013b), whereas our data show StAR in myocytes (Fig. 3A) after 4 weeks of AngII treatment; we attribute this difference to the milder and longer period of heart stress in our model. The infarcted mouse heart failed to express P450scc (Anuka et al., 2013b), and our LC-MS/MS data did not detect P450scc in stressed rat heart that expressed abundant P450c11AS and StAR. P450scc is the only enzyme known to cleave the side chain of cholesterol to produce pregnenolone and hence is required to initiate steroidogenesis (Miller and Bose, 2011; Miller, 2017). P450scc is catalytically slow, and hence it is abundant in steroidogenic tissues (Miller and Bose, 2011; Miller, 2017); it would be readily detected if it

Downloaded from jpet.aspetjournals.org at ASPET Journals on April 9, 2024

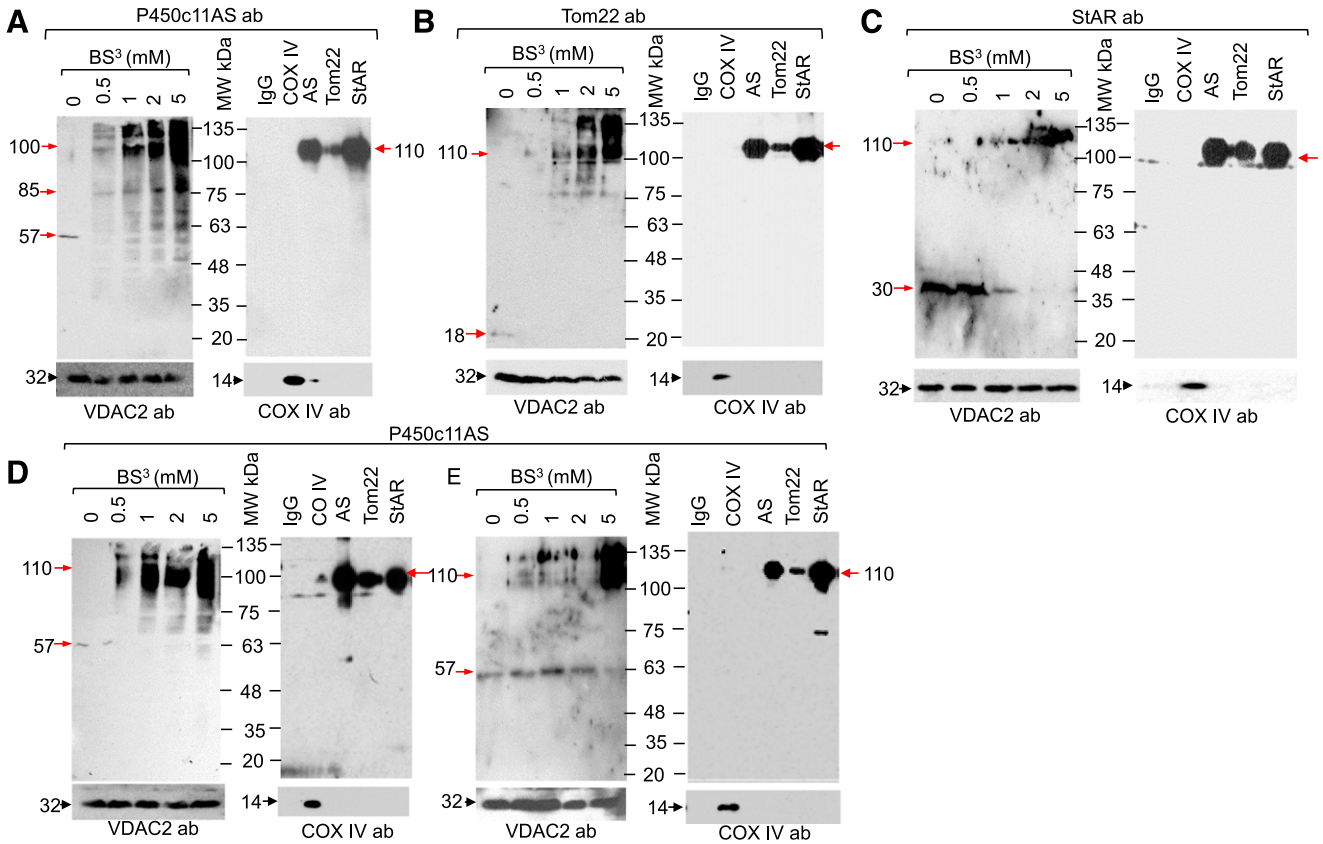

Fig. 7. Colocalization of StAR, Tom22, and P450c11AS in mitochondria by in vitro chemical crosslinking. (A–C) use 20 μg of mitochondrial protein isolated from rat heart; (D and E) use 20 μg of mitochondrial protein isolated from fresh mitochondria from H9c2 cells. In all panels, the left-hand blots show crosslinking titrations with 0–5 mM BS^3 followed by immunoblotting with anti-P450c11AS (A), anti-Tom22 (B), anti-StAR (C), and anti-P450c11AS (D and E). Blotting with anti-VDAC2 done prior to crosslinking is shown below the BS^3 titration blots showing equivalent amounts of protein loaded in each lane. The right-hand panels show coimmunoprecipitation of the 2-mM BS^3 reaction with the indicated antibodies, identifying P450c11AS (A), Tom22 (B), and StAR (C) in the 110-kDa band from rat heart mitochondria. (D and E) Identification of the interaction of P450c11AS with StAR and Tom22 in H9c2 cells. (D) Crosslinking using mitochondrial protein from H9c2 cells stimulated with AngII and immunoblotted with anti-P450c11AS; 2 mM BS^3 again gave optimal results. Right, immunoprecipitation of the 2-mM BS^3 crosslinking products with IgG, anti-COX IV (COX IV), anti-P450c11AS (AS), anti-Tom22 (Tom22), or anti-StAR (StAR) antibodies followed by immunoblotting with anti-P450c11AS. (E) Identification of interactions in H9c2 cells incubated with AngII plus siRNA against StAR and immunoblotted with anti-P450c11AS. Right, immunoprecipitation of the 2-mM BS^3 crosslinking products with IgG, anti-COX IV (COX IV), anti-P450c11AS (AS), anti-Tom22 (Tom22), or anti-StAR (StAR) antibodies. The right-hand bottom panels show immunoblotting of the co-IP experiment with COX IV antibody.

were initiating the aldosterone synthesis we detect in rat heart mitochondria. Alternatively, the substrate for cardiac P450c11AS may be a steroidal intermediate downstream from pregnenolone in the steroidogenic pathway. The physiologic substrate for P450c11AS is DOC, but circulating DOC concentrations are low in rodents, whereas corticosterone is abundant. Purified recombinant human P450c11AS can use corticosterone as substrate, albeit less efficiently than DOC (Hobler et al., 2012); the Km of P450c11AS with DOC as substrate is 2.7 ± 0.3 μM but is 28 ± 2 μM with corticosterone as substrate (Reddish and Guengerich, 2019). Rats stimulated with AngII had circulating corticosterone levels of 11 μM, which is sufficiently near the Km value to permit some aldosterone synthesis, hence we hypothesize that rat heart P450c11AS produces aldosterone from corticosterone taken up from the circulation. Corticosterone is produced abundantly and is the principal glucocorticoid in rodents but not in humans, wherein typical circulating concentrations are only 3–23 nM; this may explain earlier reports that the rat heart makes aldosterone (Silvestre et al., 1998; Takeda et al., 2000), but that the human heart does not (Kayes-Wandover and White, 2000). Studies of the stressed human heart are needed to clarify the potential role of cardiac aldosterone in human cardiovascular physiology.

Our data support and extend the observation that StAR participates in the activity of P450c11AS in the heart (Zhang et al., 2020). This is a surprising and unexpected result, because the only known function of StAR is to increase cholesterol flow from the OMM to the IMM in the adrenal and gonad (Miller and Bose, 2011; Miller, 2017). The 37-kDa StAR primary transcript performs this action using its mitochondrial leader peptide to associate with the cytoplasmic aspect of the OMM, where it undergoes conformational changes (Bose et al., 1999), which are apparently associated with the binding and discharge of cholesterol (Baker et al., 2005; Yaworsky et al., 2005; Murcia et al., 2006). StAR's activity to promote the flow of cholesterol from OMM to IMM is proportional to the time it resides on the OMM, and its mitochondrial import and cleavage to the 30-kDa intramitochondrial form terminate this activity; it is inactive in the IMS, IMM, or matrix (Bose et al., 2002; Miller and Bose, 2011) where it undergoes degradation by

Downloaded from jpet.aspetjournals.org at ASPET Journals on April 9, 2024

Lon protease (Granot et al., 2007; Bahat et al., 2014). Thus, with respect to promoting the mitochondrial influx of cholesterol to initiate steroidogenesis, the active form of StAR is the 37-kDa primary transcript (sometimes mistermed the StAR "precursor"), whereas the intramitochondrial 30-kDa StAR is inactive in promoting mitochondrial cholesterol influx.

How StAR might promote the activity of P450c11AS in the heart is not clear. Although the intramitochondrial 30-kDa form of StAR is inactive with respect to mitochondrial cholesterol import, we found that 30-kDa StAR interacts with P450c11AS and Tom22 and that its knockdown inhibits aldosterone synthesis. Tom22 traverses the OMM and reaches the IMS but not the matrix (Araiso et al., 2019; Tucker and Park, 2019), raising the topological question of how Tom22, P450c11AS, and StAR form a complex associated with the IMM. Nuclear-encoded IMM proteins may reach the IMM at OMM/IMM contact sites and not enter the IMS, undergoing signal sequence cleavage in the matrix followed by integration into the IMM (Neupert and Herrmann, 2007). P450scc, which is similar to P450c11AS, follows this pathway (Strushkevich *et al.*, 2011; Bose *et al.*, 2019) for its IMM integration (Brixius-Anderko and Scott, 2019). Thus Tom22, P450c11AS, and StAR will all be found at contact sites, and our crosslinking data show their interaction. Thus 30-kDa intramitochondrial StAR serves a novel indispensable role in the activity of intracardiac P450c11AS that is unrelated to the activity of 37-kDa StAR to promote mitochondrial cholesterol influx. Our results concerning aldosterone synthesis in the stressed heart do not indicate whether adrenal zona glomerulosa cells, which produce the preponderance of aldosterone, use a similar three-component complex of P450c11AS, Tom22, and StAR; this will require future work.

In summary, our data permit the following six conclusions: 1) aldosterone is synthesized within the stressed rat heart; 2) rat heart synthesis of aldosterone requires the classic aldosterone synthase, P450c11AS; 3) Tom22, StAR, and P450c11AS colocalize in a 290-kDa complex on the IMM of heart mitochondria; 4) StAR is required, as its absence ablated aldosterone synthesis; 5) the form of StAR required is the intramitochondrial 30-kDa form, and this is the first activity ascribed to intramitochondrial 30-kDa StAR; and 6) P450c11AS, Tom22, and StAR form a complex, but the manner in which StAR promotes the activity of P450c11AS needs further investigation.

Acknowledgments

H.S.B. thanks all members of his laboratory for helping in the completion of the project.

Authorship Contributions

Participated in research design: H.S. Bose.

Conducted experiments: H.S. Bose, Whittal, Marshall, Rajapaksha, Wang, M. Bose, Perry, Zhao.

Performed data analysis: H.S. Bose, Miller.

Wrote or contributed to the writing of the manuscript: H.S. Bose, Miller.

References

Acin-Perez R, Benador IY, Petcherski A, Veliova M, Benavides GA, Lagarrigue S, Caudal A, Vergnes L, Murphy AN, Karamanlidis G, et al. (2020) A novel approach to measure mitochondrial respiration in frozen biological samples. *EMBO J* **39**: e104073.

Adams BP and Bose HS (2012) Alteration in accumulated aldosterone synthesis as a result of N-terminal cleavage of aldosterone synthase. *Mol Pharmacol* **81**:465–474.

Anuka E, Gal M, Stocco DM, and Orly J (2013a) Expression and roles of steroidogenic acute regulatory (StAR) protein in 'non-classical', extra-adrenal and extra-gonadal cells and tissues. *Mol Cell Endocrinol* **371**:47–61.

Anuka E, Yivgi-Ohana N, Eimerl S, Garfinkel B, Melamed-Book N, Chepurkol E, Aravot D, Zinman T, Shainberg A, Hochhauser E, et al. (2013b) Infarct-induced steroidogenic acute regulatory protein: a survival role in cardiac fibroblasts. *Mol Endocrinol* **27**:1502–1517.

Araiso Y, Tsutsumi A, Qiu J, Imai K, Shiota T, Song J, Lindau C, Wenz LS, Sakaue H, Yunoki K, et al. (2019) Structure of the mitochondrial import gate reveals distinct preprotein paths. *Nature* **575**:395–401.

Bahat A, Perlberg S, Melamed-Book N, Lauria I, Langer T, and Orly J (2014) StAR enhances transcription of genes encoding the mitochondrial proteases involved in its own degradation. *Mol Endocrinol* **28**:208–224.

Baker BY, Yaworsky DC, and Miller WL (2005) A pH-dependent molten globule transition is required for activity of the steroidogenic acute regulatory protein, StAR. *J Biol Chem* **280**:41753–41760.

Benson SC, Pershadsingh HA, Ho CI, Chittiboyina A, Desai P, Pravenec M, Qi N, Wang J, Avery MA, and Kurtz TW (2004) Identification of telmisartan as a unique angiotensin II receptor antagonist with selective PPARγ-modulating activity. *Hypertension* **43**:993–1002 Publication Status.

Bose HS, Gebrail F, Marshall B, Perry EW, and Whittal RW (2019) Inner mitochondrial translocase Tim50 is central in adrenal and testicular steroid synthesis. *Mol Cell Biol* **39**:e00484-18.

Bose HS, Lingappa VR, and Miller WL (2002) Rapid regulation of steroidogenesis by mitochondrial protein import. *Nature* **417**:87–91.

Bose HS, Marshall B, Debnath DK, Perry EW, and Whittal RM (2020) Electron transport chain complex II regulates steroid metabolism. *iScience* **23**:101295.

Bose HS, Whittal RM, Baldwin MA, and Miller WL (1999) The active form of the steroidogenic acute regulatory protein, StAR, appears to be a molten globule. *Proc Natl Acad Sci USA* **96**:7250–7255.

Bose M, Whittal RM, Miller WL, and Bose HS (2008) Steroidogenic activity of StAR requires contact with mitochondrial VDAC1 and phosphate carrier protein. *J Biol Chem* **283**:8837–8845.

Brixius-Anderko S and Scott EE (2019) Structure of human cortisol-producing cytochrome P450 11B1 bound to the breast cancer drug fadrozole provides insights for drug design. *J Biol Chem* **294**:453–460.

Burson JM, Aguilera G, Gross KW, and Sigmund CD (1994) Differential expression of angiotensin receptor 1A and 1B in mouse. *Am J Physiol* **267**:E260–E267.

Cannavo A, Marzano F, Elia A, Liccardo D, Bencivenga L, Gambino G, Perna C, Rapacciuolo A, Cittadini A, Ferrara N, et al. (2019) Aldosterone jeopardizes myocardial insulin and β-adrenergic receptor signaling via G protein-coupled receptor kinase 2. *Front Pharmacol* **10**:888.

Casal AJ, Silvestre JS, Delcayre C, and Capponi AM (2003) Expression and modulation of steroidogenic acute regulatory protein messenger ribonucleic acid in rat cardiocytes and after myocardial infarction. *Endocrinology* **144**:1861–1868.

Curnow KM, Tusie-Luna MT, Pascoe L, Natarajan R, Gu JL, Nadler JL, and White PC (1991) The product of the CYP11B2 gene is required for aldosterone biosynthesis in the human adrenal cortex. *Mol Endocrinol* **5**:1513–1522.

de Gasparo M, Catt KJ, Inagami T, Wright JW, and Unger T (2000) International union of pharmacology. XXIII. The angiotensin II receptors. *Pharmacol Rev* **52**:415–472.

De Paul AL, Mukdsi JH, Petiti JP, Gutierrez S, Quintar AA, Maldonado C, and Torres A (2012) Immunoelectron microscopy: a reliable tool for the analysis of cellular processes. in *Applications of Immunocytochemistry*, pp 65–96 InTechOpen, University Campus STeP Ri, Rijeka, Croatia.

Gasc JM, Shanmugam S, Sibony M, and Corvol P (1994) Tissue-specific expression of type 1 angiotensin II receptor subtypes. An in situ hybridization study. *Hypertension* **24**:531–537.

Gewirtz H and Dilsizian V (2017) Myocardial viability: survival mechanisms and molecular imaging targets in acute and chronic ischemia. *Circ Res* **120**:1197–1212.

Gomez-Sanchez CE, Qi X, Velarde-Miranda C, Plonczynski MW, Parker CR, Rainey W, Satoh F, Maekawa T, Nakamura Y, Sasano H, et al. (2014) Development of monoclonal antibodies against human CYP11B1 and CYP11B2. *Mol Cell Endocrinol* **383**:111–117.

Granot Z, Kobiler O, Melamed-Book N, Eimerl S, Bahat A, Lu B, Braun S, Maurizi MR, Suzuki CK, Oppenheim AB, et al. (2007) Turnover of mitochondrial steroidogenic acute regulatory (StAR) protein by Lon protease: the unexpected effect of proteasome inhibitors. *Mol Endocrinol* **21**:2164–2177.

Hattangady NG, Olala LO, Bollag WB, and Rainey WE (2012) Acute and chronic regulation of aldosterone production. *Mol Cell Endocrinol* **350**:151–162.

Hobler A, Kagawa N, Hutter MC, Hartmann MF, Wudy SA, Hannemann F, and Bernhardt R (2012) Human aldosterone synthase: recombinant expression in E. coli and purification enables a detailed biochemical analysis of the protein on the molecular level. *J Steroid Biochem Mol Biol* **132**:57–65.

Huby AC, Antonova G, Groenendyk J, Gomez-Sanchez CE, Bollag WB, Filosa JA, and Belin de Chantemèle EJ (2015) Adipocyte-derived hormone leptin is a direct regulator of aldosterone secretion, which promotes endothelial dysfunction and cardiac fibrosis. *Circulation* **132**:2134–2145.

Jöhren O, Golsch C, Dendorfer A, Qadri F, Häuser W, and Dominiak P (2003) Differential expression of AT1 receptors in the pituitary and adrenal gland of SHR and WKY. *Hypertension* **41**:984–990.

Karnik SS, Unal H, Kemp JR, Tirupula KC, Eguchi S, Vanderheyden PM, and Thomas WG (2015) Angiotensin receptors: interpreters of pathophysiological angiotensinergic stimuli [published correction appears in *Pharmacol Rev* (2015) 67: 820]. *Pharmacol Rev* **67**:754–819.

Kawamoto T, Mitsuuchi Y, Toda K, Yokoyama Y, Miyahara K, Miura S, Ohnishi T, Ichikawa Y, Nakao K, Imura H, et al. (1992) Role of steroid 11β-hydroxylase and steroid 18-hydroxylase in the biosynthesis of glucocorticoids and mineralocorticoids in humans. *Proc Natl Acad Sci USA* **89**:1458–1462.

Kayes-Wandover KM and White PC (2000) Steroidogenic enzyme gene expression in the human heart. *J Clin Endocrinol Metab* **85**:2519–2525.

Downloaded from jpet.aspetjournals.org at ASPET Journals on April 9, 2024

Lin D, Sugawara T, Strauss JF 3rd, Clark BJ, Stocco DM, Saenger P, Rogol A, and Miller WL (1995) Role of steroidogenic acute regulatory protein in adrenal and gonadal steroidogenesis. *Science* **267**:1828–1831.
Lombès M, Alfaidy N, Eugene E, Lessana A, Farman N, and Bonvalet JP (1995) Prerequisite for cardiac aldosterone action. Mineralocorticoid receptor and 11 β-hydroxysteroid dehydrogenase in the human heart. *Circulation* **92**:175–182.
MacKenzie SM, Connell JMC, and Davies E (2012) Non-adrenal synthesis of aldosterone: a reality check. *Mol Cell Endocrinol* **350**:163–167.
Miller WL (2017) Disorders in the initial steps in adrenal synthesis. *J Steroid Biochem Mol Biol* **165**:18–37.
Miller WL and Auchus RJ (2011) The molecular biology, biochemistry, and physiology of human steroidogenesis and its disorders. *Endocr Rev* **32**:81–151.
Miller WL and Bose HS (2011) Early steps in steroidogenesis: intracellular cholesterol trafficking. *J Lipid Res* **52**:2111–2135.
Murcia M, Faráldo-Gómez JD, Maxfield FR, and Roux B (2006) Modeling the structure of the StART domains of MLN64 and StAR proteins in complex with cholesterol. *J Lipid Res* **47**:2614–2630.
Murphy AM, Wong AL, and Bezuhly M (2015) Modulation of angiotensin II signaling in the prevention of fibrosis. *Fibrogenesis Tissue Repair* **8**:7.
Murphy TJ, Alexander RW, Griendling KK, Runge MS, and Bernstein KE (1991) Isolation of a cDNA encoding the vascular type-1 angiotensin II receptor. *Nature* **351**:233–236.
Naghdi S and Hajnóczky G (2016) VDAC2-specific cellular functions and the underlying structure. *Biochim Biophys Acta* **1863**:2503–2514.
Naghdi S, Várnai P, and Hajnóczky G (2015) Motifs of VDAC2 required for mitochondrial Bak import and tBid-induced apoptosis. *Proc Natl Acad Sci USA* **112**: E5590–E5599.
Neupert W and Herrmann JM (2007) Translocation of proteins into mitochondria. *Annu Rev Biochem* **76**:723–749.
Ogishima T, Shibata H, Shimada H, Mitani F, Suzuki H, Saruta T, and Ishimura Y (1991) Aldosterone synthase cytochrome P-450 expressed in the adrenals of patients with primary aldosteronism. *J Biol Chem* **266**:10731–10734.
Paradis P, Dali-Youcef N, Paradis FW, Thibault G, and Nemer M (2000) Overexpression of angiotensin II type I receptor in cardiomyocytes induces cardiac hypertrophy and remodeling. *Proc Natl Acad Sci USA* **97**:931–936.
Pascoe L, Curnow KM, Slutsker L, Rösler A, and White PC (1992) Mutations in the human CYP11B2 (aldosterone synthase) gene causing corticosterone methyloxidase II deficiency. *Proc Natl Acad Sci USA* **89**:4996–5000.
Pawlak KJ, Prasad M, Thomas JL, Whittal RM, and Bose HS (2011) Inner mitochondrial translocase Tim50 interacts with 3β-hydroxysteroid dehydrogenase type 2 to regulate adrenal and gonadal steroidogenesis. *J Biol Chem* **286**:39130–39140.
Prasad M, Kaur J, Pawlak KJ, Bose M, Whittal RM, and Bose HS (2015) Mitochondria-associated endoplasmic reticulum membrane (MAM) regulates steroidogenic activity via steroidogenic acute regulatory protein (StAR)-voltage-dependent anion channel 2 (VDAC2) interaction. *J Biol Chem* **290**:2604–2616.
Prasad M, Pawlak KJ, Burak WE, Perry EE, Marshall B, Whittal RM, and Bose HS (2017) Mitochondrial metabolic regulation by GRP78. *Sci Adv* **3**:e1602038.
Prasad M, Walker AN, Kaur J, Thomas JL, Powell SA, Pandey AV, Whittal RM, Burak WE, Petruzzelli G, and Bose HS (2016) Endoplasmic reticulum stress enhances mitochondrial metabolic activity in mammalian adrenals and gonads. *Mol Cell Biol* **36**:3058–3074.
Premer C, Lamondin C, Mitzey A, Speth RC, and Brownfield MS (2013) Immunohistochemical Localization of AT1a, AT1b, and AT2 angiotensin II receptor subtypes in the rat adrenal, pituitary, and brain with a perspective commentary. *Int J Hypertens* **2013**:175428.
Psychoyos S, Tallan HH, and Greengard P (1966) Aldosterone synthesis by adrenal mitochondria. *J Biol Chem* **241**:2949–2956.
Rajapaksha M, Kaur J, Bose M, Whittal RM, and Bose HS (2013) Cholesterol-mediated conformational changes in the steroidogenic acute regulatory protein are essential for steroidogenesis. *Biochemistry* **52**:7242–7253.
Rajapaksha M, Kaur J, Prasad M, Pawlak KJ, Marshall B, Perry EW, Whittal RM, and Bose HS (2016) An outer mitochondrial translocase, Tom22, is crucial for inner mitochondrial steroidogenic regulation in adrenal and gonadal tissues. *Mol Cell Biol* **36**:1032–1047.
Reddish MJ and Guengerich FP (2019) Human cytochrome P450 11B2 produces aldosterone by a processive mechanism due to the lactol form of the intermediate 18-hydroxycorticosterone. *J Biol Chem* **294**:12975–12991.
Robert V, Heymes C, Silvestre J-S, Sabri A, Swynghedauw B, and Delcayre C (1999) Angiotensin AT1 receptor subtype as a cardiac target of aldosterone: role in aldosterone-salt-induced fibrosis. *Hypertension* **33**:981–986.
Rocha R, Rudolph AE, Frierdich GE, Nachowiak DA, Kekec BK, Blomme EA, McMahon EG, and Delyani JA (2002) Aldosterone induces a vascular inflammatory phenotype in the rat heart. *Am J Physiol Heart Circ Physiol* **283**:H1802–H1810.
Rocha R, Stier CT Jr, Kifor I, Ochoa-Maya MR, Rennke HG, Williams GH, and Adler GK (2000) Aldosterone: a mediator of myocardial necrosis and renal arteriopathy. *Endocrinology* **141**:3871–3878.
Rosenfeld J, Capdevielle J, Guillemot JC, and Ferrara P (1992) In-gel digestion of proteins for internal sequence analysis after one- or two-dimensional gel electrophoresis. *Anal Biochem* **203**:173–179.
Schnee JM and Hsueh WA (2000) Angiotensin II, adhesion, and cardiac fibrosis. *Cardiovasc Res* **46**:264–268.
Schupp M and Unger T (2005) Telmisartan: from lowering blood pressure to end-organ protection. *Future Cardiol* **1**:7–15.
Silvestre JS, Robert V, Heymes C, Aupetit-Faisant B, Mouas C, Moalic JM, Swynghedauw B, and Delcayre C (1998) Myocardial production of aldosterone and corticosterone in the rat. Physiological regulation. *J Biol Chem* **273**:4883–4891.
Slight SH, Ganjam VK, Gómez-Sánchez CE, Zhou MY, and Weber KT (1996) High affinity NAD(+)-dependent 11 β-hydroxysteroid dehydrogenase in the human heart. *J Mol Cell Cardiol* **28**:781–787.
Strushkevich N, MacKenzie F, Cherkesova T, Grabovec I, Usanov S, and Park HW (2011) Structural basis for pregnenolone biosynthesis by the mitochondrial monooxygenase system. *Proc Natl Acad Sci USA* **108**:10139–10143.
Swartz ME (1991) Method development and selectivity control for small molecule pharmaceutical separations by capillary electrophoresis. *J Liq Chromatogr* **14**: 923–928.
Takeda Y, Yoneda T, Demura M, Miyamori I, and Mabuchi H (2000) Cardiac aldosterone production in genetically hypertensive rats. *Hypertension* **36**:495–500.
Tucker K and Park E (2019) Cryo-EM structure of the mitochondrial protein-import channel TOM complex at near-atomic resolution. *Nat Struct Mol Biol* **26**:1158–1166.
Walker BR, Yau JL, Brett LP, Seckl JR, Monder C, Williams BC, and Edwards CRW (1991) 11 β-hydroxysteroid dehydrogenase in vascular smooth muscle and heart: implications for cardiovascular responses to glucocorticoids. *Endocrinology* **129**: 3305–3312.
Welch BL (1947) The generalisation of student's problems when several different population variances are involved. *Biometrika* **34**:28–35.
Yaworsky DC, Baker BY, Bose HS, Best KB, Jensen LB, Bell JD, Baldwin MA, and Miller WL (2005) pH-dependent Interactions of the carboxyl-terminal helix of steroidogenic acute regulatory protein with synthetic membranes. *J Biol Chem* **280**:2045–2054.
Ye P, Kenyon CJ, MacKenzie SM, Jong AS, Miller C, Gray GA, Wallace A, Ryding AS, Mullins JJ, McBride MW, et al. (2005) The aldosterone synthase (CYP11B2) and 11β-hydroxylase (CYP11B1) genes are not expressed in the rat heart. *Endocrinology* **146**:5287–5293.
Zhang L-H, Pang X-F, Bai F, Wang N-P, Shah AI, McKallip RJ, Li X-W, Wang X, and Zhao Z-Q (2015) Preservation of glucagon-like peptide-1 level attenuates angiotensin II-Iinduced tissue fibrosis by altering AT1/AT2 receptor expression and angiotensin-converting enzyme 2 activity in rat heart. *Cardiovasc Drugs Ther* **29**: 243–255.
Zhang WW, Zheng RH, Bai F, Sturdivant K, Wang NP, James EA, Bose HS, and Zhao ZQ (2020) Steroidogenic acute regulatory protein/aldosterone synthase mediates angiotensin II-induced cardiac fibrosis and hypertrophy. *Mol Biol Rep* **47**:1207–1222.

Address correspondence to: Himangshu S. Bose, Mercer U School of Medicine, Memorial University Medical Center, Hoskins Research Bldg., 1250 East 66th St. Savannah, GA 31404. E-mail: bose_hs@mercer.edu

Downloaded from jpet.aspetjournals.org at ASPET Journals on April 9, 2024